KIF17 Dynamics and Regulation of NR2B Trafficking in Hippocampal Neurons

Laurent Guillaud, Mitsutoshi Setou, and Nobutaka Hirokawa
Department of Cell Biology and Anatomy, Graduate School of Medicine, University of Tokyo, Bunkyo-ku Tokyo 113-0033, Japan

KIF17, a recently characterized member of the kinesin superfamily proteins, has been proposed to bind *in vitro* to a protein complex containing mLin10 (Mint1/X11) and the NR2B subunit of the NMDA receptors (NMDARs). In the mammalian brain, NMDARs play an important role in synaptic plasticity, learning, and memory. Here we present, for the first time, the dynamic properties of KIF17 and provide evidence of its function in the transport of NR2B in living mammalian neurons. KIF17 vesicles enter and move specifically along dendrites in a processive way, at an average speed of 0.76 μm/sec. These vesicles are effectively associated with extrasynaptic NR2B, and thus they transport and deliver NR2B subunits in dendrites. However, KIF17 does not seem to enter directly into postsynaptic regions. Cellular knockdown or functional blockade of KIF17 significantly impairs NR2B expression and its synaptic localization. Interestingly, the decrease in the number of synaptic NR2B subunits is followed by a parallel increase in the number of NR2A subunits at synapses. In contrast, upregulation of the expression level of NR2B, after treatment with the NMDAR antagonist D(−)-2-amino-5-phosphonopentanoic acid, simultaneously increases the expression level of KIF17. These observations concerning the downregulation or upregulation of KIF17 and NR2B reveal the probable existence of a shared regulation process between the motor and its cargo. Taken together, these results illustrate the complex mechanisms underlying the active transport and regulation of NR2B by the molecular motor KIF17 in living hippocampal neurons.

Key words: **KIF17; kinesin; NR2B; NMDA receptor; hippocampal neuron; mLin10; YFP; dynamics; regulation; antisense oligonucleotides; dominant negative; AP-V**

Introduction

In highly polarized cells such as neurons, sorting and delivery of organelles depend on the kinesin superfamily proteins (KIFs) (Hirokawa, 1996, 1998). Defects in KIFs impair neuronal functions such as action potential propagation or neurotransmitter release (Gho et al., 1992; Zhao et al., 2001). Although extensive research to discover and characterize new KIFs has been performed *in vitro* (Nakagawa et al., 1997; Yang et al., 1997, Miki et al., 2001), little is known about the real-time dynamic properties and functions of motor proteins in living mammalian neurons.

KIF17, a homodimeric motor protein with an N-terminal motor domain, belongs to the Osm-3/KIF17 family. *In vitro*, KIF17 has been shown to bind specifically through its tail domain to the postsynaptic density-95/disc large/zona occludens-1 (PDZ) domain of mLin10 within a large scaffolding protein complex that also contains the NR2B subunit of the NMDA receptor (NMDAR) (Setou et al., 2000).

mLin10 is a shared component of the polarized protein localization pathways in neurons and epithelia (Rongo et al., 1998) and is detectably expressed only in neurons (Okamoto and Sudhof, 1997). It is composed of a variable N-terminal region and a constant C-terminal region that contains two PDZ domains, one of which binds to KIF17.

NMDARs, a subtype of glutamate receptors, are oligomeric ligand-gated ion channel complexes formed by the assembly of different subunits (Moriyoshi et al., 1991). NMDAR consists of an essential subunit, NR1 (Forrest et al., 1994), and various modulatory NR2 subunits (NR2A, NR2B, NR2C, and NR2D) (Kutsuwada et al., 1992; Monyer et al., 1992). The NMDAR channel is important for synaptic plasticity, circuit development, learning, and memory (Bliss and Collingridge, 1993; Sakimura et al., 1995; Tsien et al., 1996). The NR2B subunit is essential for the synaptic localization of the NMDAR channel (Mori et al., 1998) and is directly involved in the enhancement of learning and memory in mice (Tang et al., 1999).

This work was undertaken to characterize the dynamic properties of KIF17 in living mammalian neurons. Moreover, the transport of NR2B by KIF17, as proposed by Setou et al. (2000), should be assessed to determine whether it functions *in vivo*. In addition, we wanted to analyze the effects of KIF17 inhibition on NR2B trafficking. Excluding the notion that KIF17 may transport NR2B, what other relations exist between the motor and its cargo? Here we present the first report concerning the dynamics of KIF17 in living hippocampal neurons. KIF17 moves in a vesicular form and these vesicles are effectively associated with NR2B and thus transport the subunit within dendrites. Furthermore, overexpression of KIF17 leads to a clear redistribution of the scaffolding protein mLin10, thought to be involved in the binding with NR2B. Inhibition of KIF17 activity by cellular knockdown or dominant-negative mutation decreases the NR2B ex-

Received April 26, 2002; revised Oct. 10, 2002; accepted Oct. 10, 2002.

This work was supported by Center of Excellence grants from the Ministry of Education, Culture, Science, Sports and Technology of Japan to N.H.; L.G. was supported by the Japan Society for the Promotion of Science and by the Inoue Foundation for Science. We thank Dr. M. Mishina for NR2B cDNA and Dr. M. Okamoto for Mint1 cDNA, M. Sugaya-Otsuka for technical assistance, Dr. Y. Okada for helpful comments, and Dr. H. Miki for critical reading of this manuscript.

Correspondence should be addressed to Prof. Nobutaka Hirokawa, Department of Cell Biology and Anatomy, Graduate School of Medicine, University of Tokyo, 7-3-1 Hongo, Bunkyo-ku Tokyo 113-0033, Japan. E-mail: hirokawa@m.u-tokyo.ac.jp.

Copyright © 2002 Society for Neuroscience 0270-6474/02/220131-●$15.00/0

pression level and alters its synaptic localization. However, the loss of NR2B is compensated by an increase in the number of NR2A subunits at synapses. Additionally, pharmacological stimulation of NR2B also stimulates KIF17 expression and demonstrates once more the regulatory connections between the expression of the motor and its cargo. Finally, KIF17-mediated NR2B transport appears to be one of the key regulators of NMDAR formation in hippocampal neurons.

Materials and Methods

Cell cultures. NIH 3T3 cells were grown in DMEM (Invitrogen, Rockville, MD) supplemented with 10% fetal calf serum (FCS) and subcultured every 3 d. Dissociated hippocampal neurons were prepared as described previously (Goslin and Banker, 1991). Briefly, hippocampus was removed from 16-d-old embryo mouse brains and dissociated with 0.25% trypsin. Hippocampal neurons were then plated on glass coverslips or plastic Petri dishes previously coated with poly-L-lysine (Sigma, St. Louis, MO). The culture medium used was MEM (Invitrogen), supplemented with 1 mM sodium pyruvate, 0.6 gm/l glucose, and B27 supplement mixture (Invitrogen).

Antibodies. The primary antibodies used in this study were KIF17 polyclonal antibody (pAb) (Setou et al., 2000), KIF5B pAb (Kanai et al., 2000), KIF1A pAb (our laboratory), NR2B monoclonal antibody (mAb), mLin10 mAb, postsynaptic density-95 (PSD95) mAb (BD Transduction Laboratories, Lexington, KY), NR2A, NR2B, and NR2C pAbs (Molecular Probes, Eugene, OR), GluR1 pAb (Calbiochem, San Diego, CA), synaptophysin mAb, tubulin DM1A mAb, NF-H mAb (clone NE14), and MAP2 mAb (Sigma). The Alexa568 fluorescent secondary antibodies used were from Molecular Probes, and the Cy5 fluorescent secondary antibodies were from Amersham Biosciences (Buckinghamshire, UK).

Transfection and expression of tagged proteins. Yellow fluorescent protein (YFP)-KIF17, YFP-mLin10, and YFP-NR2B expression vectors were constructed using pEYFP vectors (Clontech, Palo Alto, CA), and the hemagglutinin (HA)-KIF17 expression vectors were constructed using the pHM6 vector (Roche Molecular Biochemicals, Basel, Switzerland). Additional YFP-KIF17 and dominant-negative YFP-610 (KIF17 without motor domain) expression vectors were produced using the Sindbis virus system (Invitrogen, Carlsbad, CA). cDNA was purified using the EndoFree plasmid maxikit (Qiagen, Hilden, Germany). NIH 3T3 cells were transfected using Lipofectamin 2000 (Invitrogen) according to the manufacturer's instructions. Transfection of hippocampal neurons was performed using an optimized calcium phosphate protocol (Kohrmann et al., 1999a) or the Sindbis virus system.

Immunofluorescence. For immunofluorescence analysis, cells (NIH 3T3 or hippocampal neurons) grown on glass coverslips were fixed in PBS containing 4% paraformaldehyde, 4% sucrose, 0.1% glycerol, and 0.01% digitonin for 30 min at 37°C, and then permeabilized or not with PBS/0.005% Triton X-100 for 3 min at room temperature. The cells were further washed in PBS and blocked in PBS/3% bovine serum albumin (BSA) for 15 min at room temperature. Primary antibodies were diluted in PBS/1% BSA and incubated for 1 hr at room temperature. After three washes in PBS, cells were incubated with corresponding Alexa568 fluorescent secondary antibodies diluted in PBS/1% BSA for 1 hr at room temperature. Finally, the cells were washed three times in PBS and mounted in an antifade reagent (Molecular Probes). The cells were observed, and images were acquired with an LSM510 confocal laser-scanning microscope (Carl Zeiss, Oberkochen, Germany) and then processed using Photoshop 6.0 (Adobe, San Jose, CA).

Fluorescence recovery after photobleaching and real-time imaging of YFP-KIF17. After 9 d of culture, hippocampal neurons were exposed to 100 μM D(−)-2-amino-5-phosphonopentanoic acid (AP-V) and then transfected with YFP-KIF17 cDNA on day 10. For observation of living cells, glass coverslips were directly mounted upside down on a glass slide covered with parafilm mold filled with a drop of warm culture medium and observed under an LSM510 confocal laser-scanning microscope. Living hippocampal neurons expressing YFP-KIF17 were first located on the coverslip. A 15 μm area on the apical dendrite was bleached by 25 scans of argon/krypton laser at full power. The fluorescence recovery was then monitored over time, and images were acquired every 5 sec. Movement of individual vesicles was followed in other dendrites of the same transfected neuron, and images were acquired every 3 sec. Determination of YFP-KIF17 velocity was performed using high frame-rate acquisition (one frame per second) for 30 sec. The path of individual vesicles was traced, and distances were evaluated directly using LSM510 software. Finally, all images were processed using Photoshop 6.0 and further edited as a video file using Premiere 6.0 (Adobe). The analysis and graphical representation of fluorescence recovery after photobleaching (FRAP) experiments were performed using ImageJ (National Institutes of Health, Bethesda, MD) and Excel (Microsoft Corporation, Redmond, WA).

Three-dimensional reconstruction. Hippocampal neurons expressing YFP-KIF17 were processed for immunostaining of PSD95, as described above. Neurons were further observed under an LSM510 confocal laser-scanning microscope. Thirty Z sections were acquired to produce a stack that was then rendered using Autodeblur and Autovisualize software (Autoquant Imaging, Watervliet, NY) to obtain three-dimensional (3D) images and animations.

Pharmacological treatment. Cerebral hemispheres from 16-d-old mouse embryos were dissected and incubated in HBSS with 0.25% trypsin for 15 min at 37°C. Cells were passed through nylon mesh, centrifuged for 5 min at 1500 rpm, and resuspended in HBSS. Dissociated hippocampal neurons were then added to the suspension in a 2:1 ratio. The resulting cell suspension was finally plated on plastic Petri dishes previously coated with poly-L-lysine. Cells were grown for 3 d in B27-supplemented medium at 37°C in 5% CO_2 atmosphere before stimulation. The NMDAR antagonist AP-V at 100 μM or the AMPA-type glutamate receptor antagonist 6-cyano-7-nitroquinoxaline-2, 3-dione (CNQX) at 10 μM was added to neuronal cultures in MEM medium containing 100 μM L-glutamine, 5% horse serum, 5% FCS, 33.3 mM glucose, 26.2 mM $NaHCO_3$, and B27 supplement mixture. Stimulation medium was changed daily for 7 d.

Cellular knockdown of KIF17. The antisense oligonucleotide against KIF17 cDNA used in this study was 5′-CAGAGGCTCACCACCGAA-3′, and the corresponding sense oligonucleotide was 5′-TTCGGTGGTGAGCCTCTG-3′. All oligonucleotides were synthesized with a phosphothiorate group on each residue. In some experiments, fluorescent (FITC tag in 5′) oligonucleotides were used. The oligonucleotides were added directly to the culture medium, and cultures were checked after 6 hr–3 d of treatment. For Western blot analysis, 1 μM oligonucleotides was added on days 3–5 of culture. The medium containing the oligonucleotides was replaced every day during the treatment. For immunofluorescence analysis, hippocampal neurons were treated with 1 μM FITC-tagged oligonucleotides for 6–24 hr before fixation and observation.

Western blot analysis. Cultured hippocampal neurons were washed twice in PBS and scraped in boiling sample buffer (Laemmli, 1970), boiled again for 3 min, and loaded into SDS-polyacrylamide gel for electrophoresis. Proteins were transferred onto a polyvinylidene difluoride Immobilon membrane (Ambion, Austin, TX) and probed with specific primary antibodies and corresponding horseradish peroxidase-conjugated secondary antibodies. Detection was performed using electrochemiluminescence (ECL) according to the manufacturer's instructions (Amersham Biosciences). The membranes were then exposed to Hyperfilm ECL (Amersham Biosciences). Films were digitally scanned; signals were quantified using ImageJ, and data were plotted with Excel.

Results

The present work was undertaken to determine the dynamics of the molecular motor KIF17 and the transport and targeting of NR2B in neurons. Transfection and overexpression of green fluorescent protein (GFP)-tagged proteins have been widely used to study dynamic processes (Fischer et al., 1998; Craven et al., 1999; Kohrmann et al., 1999b; Okabe et al., 1999; Prekeris et al., 1999; Shi et al., 1999; Burack et al., 2000). Here we used YFP-tagged KIF17, mLin10, and NR2B, hemagglutinin-tagged KIF17 (HA-KIF17), and YFP-610, the dominant-negative form of KIF17 (deletion of the motor domain: aa 1 to aa 309), to determine

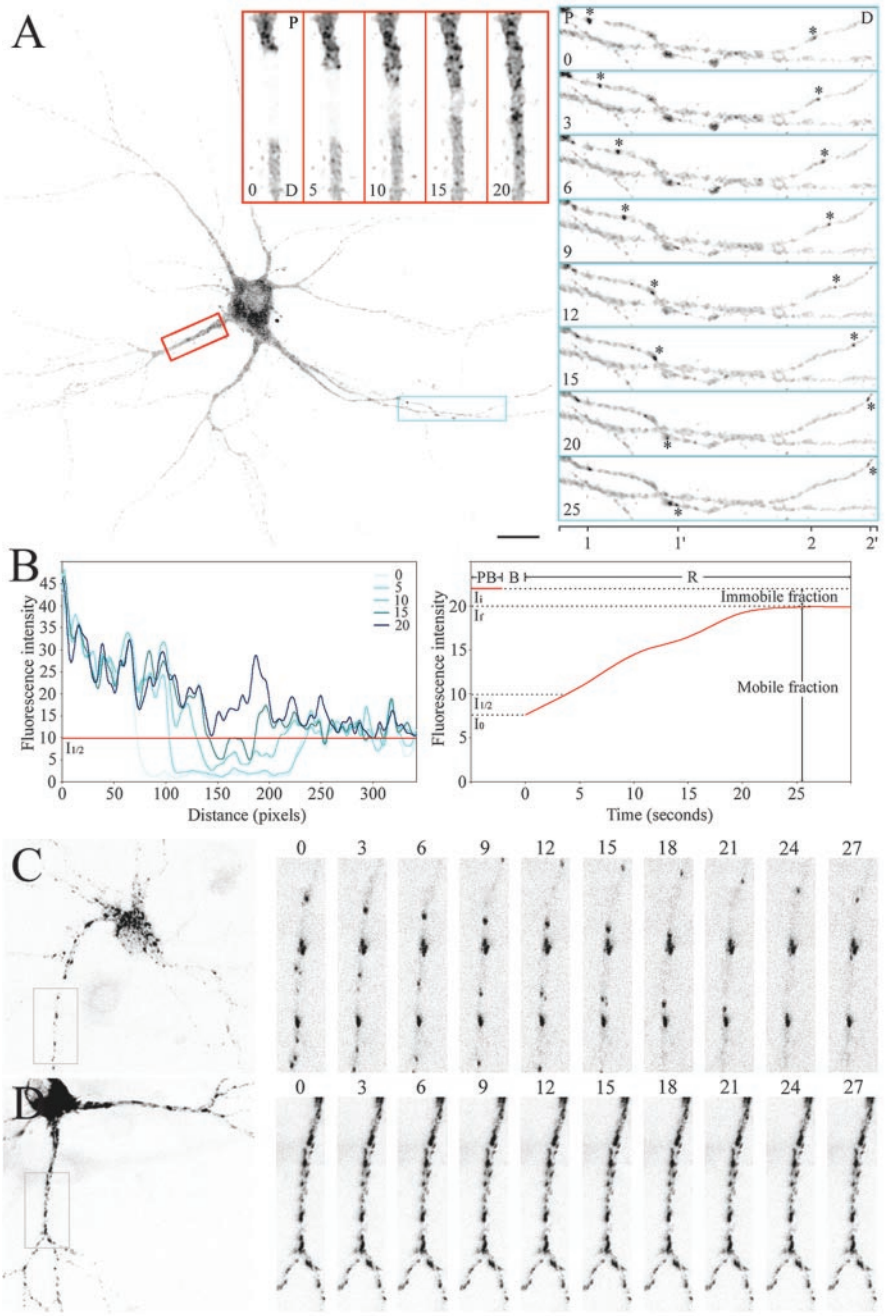

Figure 1. Dynamic properties of YFP-KIF17 in living hippocampal neurons. Hippocampal neurons cultured for 10 d were transfected with YFP-KIF17. After 24 hr, the living cells were observed under a confocal laser-scanning microscope. All images were inverted to improve visibility. *A*, Fluorescence imaging of FRAP and movement of YFP-KIF17 in transfected neurons. A 15 μm area on the apical dendrite (*red inset*) was bleached, and the fluorescence recovery was monitored every 5 sec. Recovery was achieved from both the proximal part (*P*) and the distal part (*D*) of the bleached area. Small vesicular structures moved within the area, and fluorescence was completely restored after 20 sec. Movement of individual YFP-KIF17 vesicles was also monitored over time in another dendrite of the same neuron (*blue inset*). Images were taken every 3 sec and show the movement of two vesicles (*) from the proximal (*P*) to the distal (*D*) part of the dendrite. Initial positions *1* and *2* and final positions *1′* and *2′* of both vesicles were plotted below. Scale bar, 20 μm. *B*, Graphic analysis of FRAP experiments. Shown is a plot profile of the fluorescence intensity as a function of the distance in the bleached area (*left panel*). An increasing number of fluorescence peaks corresponding to vesicular structures of YFP-KIF17 appeared in the bleached area. Mean fluorescence intensity as a function of time plotted on the *right panel* shows the initial fluorescence intensity (*Ii*), the fluorescence intensity right after bleaching (*I0*), the final fluorescence intensity (*If*) after complete recovery, and the half fluorescence intensity (*I1/2*). *PB*, Prebleach; *B*, bleach; *R*, recovery. *C*, High frame-rate acquisition of a transfected hippocampal neuron expressing YFP-KIF17. Several vesicles moved anterogradely, whereas few aggregates were immobile. *D*, High frame-rate acquisition of a transfected hippocampal neuron expressing YFP-KIF17 and treated with 20 μM nocodazole for 45 min. The movement of YFP-KIF17 is inhibited completely. Increasing numbers of immobile aggregates can be observed both in dendrites and in the cell body.

their localization, distribution, and inter-relationship in living hippocampal neurons.

Dynamic properties of YFP-KIF17 in cultured hippocampal neurons

To understand the physiological role of KIF17 *in vivo*, we first needed to fully characterize its dynamic properties in living neurons.

Velocity and directionality of YFP-KIF17

Hippocampal neurons cultured for 10 d were transfected with YFP-KIF17 using the calcium phosphate method or Sindbis virus. Six to 24 hr after transfection, living neurons were observed under a confocal laser-scanning microscope. We first determined the dynamic properties of KIF17 using FRAP and real-time imaging of YFP-KIF17. An example of a transfected neuron expressing YFP-KIF17 is shown in Figure 1*A*. We bleached a 15 μm area in the proximal region of the apical dendrite and monitored the fluorescence recovery of the bleached region every 5 sec (Fig. 1*A*, *red inset*). The recovery started 5–10 sec after bleaching. Fluorescence in the bleached region was fully restored after 20–30 sec (video 1, supplemental data; available at www.jneurosci.org), and the average velocity, determined experimentally for the total recovery process, was 0.78 ± 0.22 μm/sec. However, the fluorescence recovery occurred on both sides of the bleached region, indicating that YFP-KIF17 has both anterograde and retrograde movement within the proximal dendrite. Analysis of the FRAP experiment is shown in Figure 1*B*. The velocities for the proximal and distal movements were calculated according to Figure 1*B* for $I_{1/2}$ and were found to be 0.71 ± 0.18 and 0.30 ± 0.12 μm/sec, respectively ($n = 10$). The recovery from the proximal part was faster and more effective than the one from the distal part of the dendrite. The plot profile in Figure 1*B*, *left panel*, shows an increasing number of fluorescence peaks (corresponding to highly fluorescent vesicles moving in the area as observed in Fig. 1*A*, *red inset*). The mobile and immobile fractions of YFP-KIF17 were determined by plotting the fluorescence intensity as a function of time, as shown in Figure 1*B*, *right panel* (for review, see White and Stelzer, 1999). According to these calculations, 88.34 ± 0.36% of YFP-KIF17 was mobile, whereas 11.41 ± 0.80% remained immobile. We also monitored the movement of individual vesicles in the distal region of another dendrite on the same neurons (Fig. 1*A*,

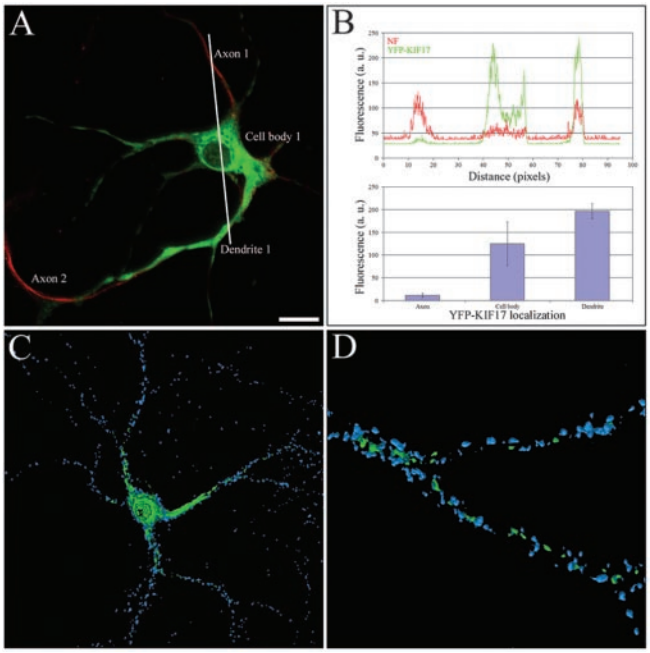

Figure 2. Distribution of YFP-KIF17 in hippocampal neurons. *A*, Dendritic localization of YFP-KIF17. Transfected hippocampal neurons were immunostained with anti-phosphorylated-NF-H mAb to discriminate axon (*red*) from dendrites. YFP-KIF17 (*green*) localizes mainly in dendrites and the cell body. Scale bar, 20 μm. *B*, Quantitative analysis of the axo/dendritic distribution of YFP-KIF17. The fluorescence intensity profile showing YFP-KIF17 (*green*) and NF-H (*red*) was measured using the fluorescence profile function of LSM510 software on an *x–z* plane following the line to obtain a profile containing cross sections of the axon, the cell body, and the dendrite at the same time. *C*, *D*, Three-dimensional reconstruction images of hippocampal neurons expressing YFP-KIF17. Ten-day-old cultures were transfected with YFP-KIF17 (*green*) and processed for immunodetection of synaptic clusters using anti-PSD95 mAb (*blue*). Rendering of 3D images from confocal Z stacks files was performed using Autodeblur and Autovisualize. YFP-KIF17 is fully restricted to the dendritic shaft and did not enter in postsynaptic regions.

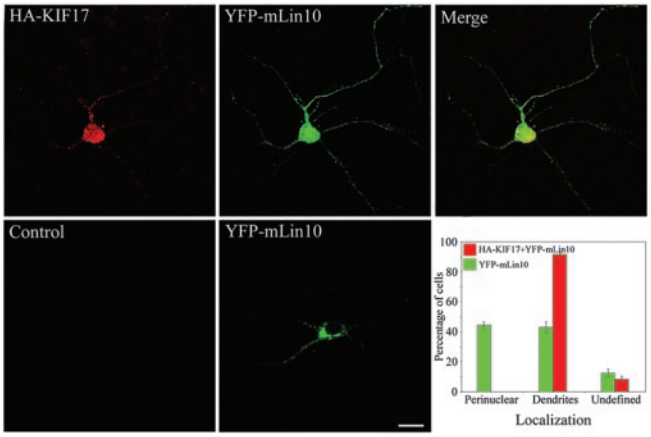

Figure 3. Distribution of YFP-mLin10 in HA-KIF17-cotransfected hippocampal neurons. After 10 d of culture, hippocampal neurons were cotransfected with HA-KIF17 and YFP-mLin10. Twenty-four hours after transfection, the cells were fixed (see Materials and Methods), and HA-KIF17 was detected with the Alexa568 fluorescent secondary antibody. Overexpression of HA-KIF17 (*red*) induced a clear redistribution of YFP-mLin10 (*green*) from its initial perinuclear localization (as observed in control single-transfected cells) to the dendritic network. Scale bar, 20 μm. Statistical analysis of the redistribution of YFP-mLin10 in hippocampal neurons shows the percentage of cells with perinuclear or dendritic localization of YFP-mLin10 in single-transfected cells or HA-KIF17 cotransfected cells. *Undefined* corresponds to an unclear pattern with both perinuclear and dendritic localizations of the proteins.

blue inset). The movement of two vesicles (vesicles 1 and 2) was easily monitored toward the tip of the dendrite. The velocities of the vesicles were 0.70 and 0.45 μm/sec for vesicles 1 and 2, respectively. We then determined the average velocity of a single vesicle on nonbleached neurons using high frame-rate acquisition (Fig. 1*C*). Several individual vesicles moved anterogradely along the dendrites, whereas some aggregates accumulated in some distinct regions of the dendrites (video 2, supplemental data). The velocity of a single vesicle was 0.76 $\pm$ 0.31 μm/sec (n = 30). No movement was observed in hippocampal neurons treated with the microtubule-depolymerizing drug nocodazole (Fig. 1*D*), showing that the integrity of the microtubule network is required for the movement of the microtuble-dependent molecular motor KIF17. Accumulation of YFP-KIF17 aggregates was also clearly observed in the soma and dendrites of hippocampal neurons exposed to nocodazole (Fig. 1*D*) compared with those of untreated neurons (Fig. 1*C*). Moreover, no fluorescence recovery or vesicle movement was observed in hippocampal neurons exposed to low temperatures, which also depolymerized microtubules (data not shown).

Polarity and distribution of YFP-KIF17

The expression pattern and localization of YFP-KIF17 were similar to those observed for the endogenous KIF17 (Fig. 1, supplemental data). In addition, the overexpression of YFP-KIF17 was still in the range and compatible with the expression level of the endogenous KIF17 as shown by immunofluorescence (Fig. 1, supplemental data). YFP-KIF17 overexpression increased the expression level of KIF17 by 1.3-fold. We further investigated the distribution of YFP-KIF17 in transfected neurons. Hippocampal neurons expressing YFP-KIF17 were immunostained with the antiphosphorylated neurofilament antibody to discriminate between axon and dendrites. We observed that YFP-KIF17 enters dendrites preferentially (Fig. 2*A*). Quantification shows that 3% of YFP-KIF17 is in the axon, whereas 59% is in the dendrite and 38% remains in the cell body (Fig. 2*B*). The axo/dendritic ratio of YFP-KIF17 is 0.05. These results are in agreement with the data obtained for the endogenous KIF17 (1% in axon, 64% in dendrite, and 35% in cell body, and an axo/dendritic ratio of 0.02). In addition, we determined the precise localization of YFP-KIF17 vesicles in the dendrites of transfected neurons using 3D reconstruction. Neurons expressing YFP-KIF17 were immunostained with the PSD95 antibody and processed for Z series acquisition under a confocal laser-scanning microscope. Three-dimensional reconstruction images and animations clearly showed that YFP-KIF17 vesicles are not colocalized with PSD95 clusters (Fig. 2*C*,*D*) (video 3, supplemental data). We also immunostained YFP-KIF17-transfected neurons with PSD95 and NR2B, or synaptophysin and NR2B. However, we did not observe any colocalization of YFP-KIF17 and PSD95 or of YFP-KIF17 and synaptophysin, indicating that YFP-KIF17 vesicles are effectively restricted to the dendritic shaft and do not enter postsynaptic regions (see Fig. 4*C*,*D*).

Start and end of YFP-KIF17 movement

We have shown that YFP-KIF17 enters and moves into the dendrites of transfected neurons. However, vesicles seem to stop their movements within the shaft of the dendrites in several locations where YFP-KIF17 seems to accumulate in a stationary state (Fig. 1*A*,*C*) (video 2, supplemental data). Surprisingly, no significant accumulation of KIF17 vesicles at the tip of dendrites was observed.

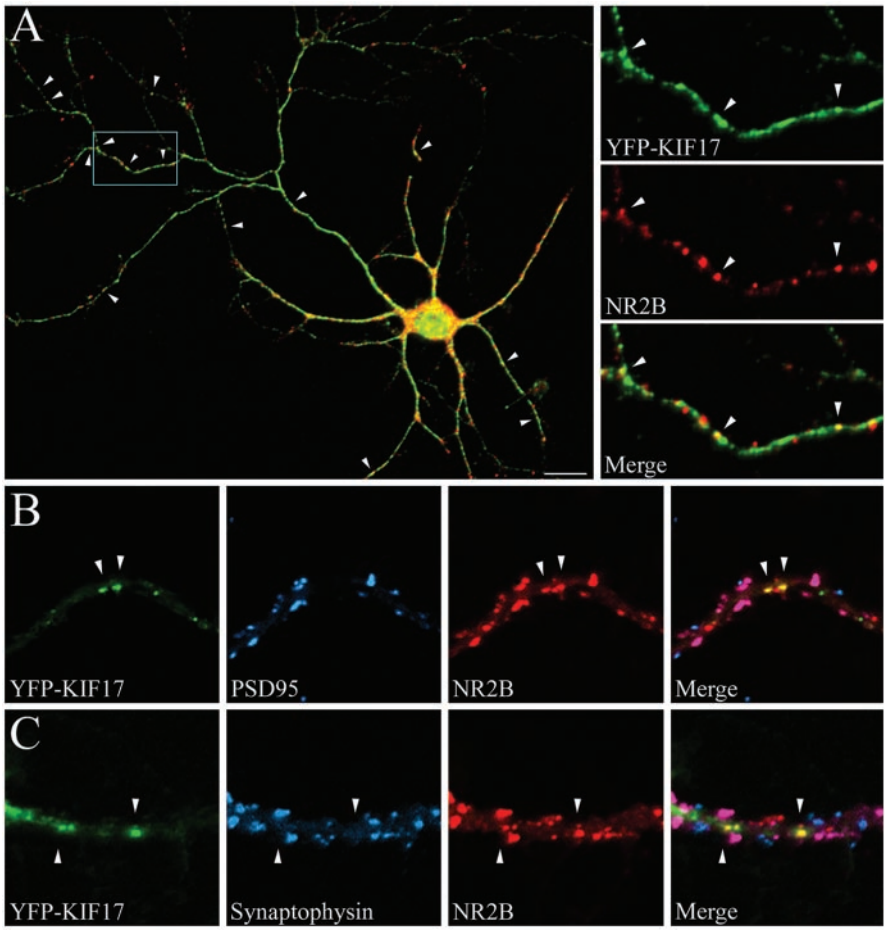

Figure 4. Colocalization of YFP-KIF17 and NR2B. After 10 d of culture, hippocampal neurons were transfected with YFP-KIF17, and living cells were observed under a confocal laser-scanning microscope. Vesicular movement of YFP-KIF17 was first verified in the transfected neurons. The cells were then fixed, and immunodetection was performed as described in Materials and Methods. *A*, Transfected neuron showing YFP-KIF17 (*green*) and NR2B mAb (*red*). Shown is colocalization (*yellow*) of YFP-KIF17 and NR2B on the same vesicles (*arrowheads*). Higher magnification is shown in the *blue inset*. Scale bar, 20 μm. *B*, *C*, Localization of extrasynaptic and synaptic NR2B clusters. Hippocampal neurons expressing YFP-KIF17 (*green*) were permeabilized and immunostained (see Materials and Methods) for PSD95 mAb (*blue*) and NR2B pAb (*red*) (*B*) or synaptophysin mAb (*blue*) and NR2B pAb (*red*) (*C*). The mobile extrasynaptic NR2B subunits colocalize with YFP-KIF17 vesicles (*yellow* and *arrowheads*), whereas the immobile synaptic NR2B subunits colocalize with PSD95 or synaptophysin (*pink*). No colocalization of YFP-KIF17, PSD95, and NR2B or synaptophysin and NR2B was observed.

Redistribution of mLin10 by KIF17

We finally determined the effect of HA-KIF17 cotransfection on the localization of YFP-mLin10. Hippocampal neurons were double-transfected with HA-KIF17/YFP-mLin10. After 24 hr of transfection, cells were fixed, and HA-KIF17 was detected with the anti-HA primary antibody and Alexa568-conjugated secondary antibody. An example of a neuron coexpressing HA-KIF17/YFP-mLin10 is shown in Figure 3. When neurons expressed both HA-KIF17 and YFP-mLin10, the perinuclear staining of YFP-mLin10, observed in control single-transfected cells, redistributed to the cell body and the dendritic network (Fig. 3). We observed similar results in 3T3 cells cotransfected with HA-KIF17/YFP-mLin10 (data not shown).

Taken together, the above data clearly establish the dynamic properties of KIF17 in living neurons. KIF17 vesicles move in a plus-end microtubule direction in dendrites of living hippocampal neurons. Although this movement is essentially anterograde in the distal dendrite, a retrograde movement can occur in the proximal dendrite as a result of the presence of a mixed population of microtubules in that specific region of the dendrite. As expected, these movements are microtubule dependent because they disappear in the absence of microtubules. Moreover, KIF17 vesicles move and stop only in the shaft of dendrites without entering postsynaptic regions. In addition, these data also provide strong evidence of the transport of mLin10 by KIF17 and the interaction between these proteins in living hippocampal neurons.

Colocalization and transport of NR2B by YFP-KIF17

To determine whether YFP-KIF17 moving vesicles effectively transport NR2B, we performed immunocytochemistry on cells transfected with YFP-KIF17. After checking the movement of vesicles, cells were fixed and immunostained with anti-NR2B antibodies. YFP-KIF17 vesicles were colocalized with extrasynaptic NR2B clusters within the dendrites of transfected neurons (Fig. 4*A*). To discriminate between the moving fraction and the synaptic clusters of NR2B, we double-stained the YFP-KIF17-expressing neurons with anti-NR2B and anti-PSD95 antibodies, or with anti-NR2B and anti-synaptophysin antibodies. As shown in Figure 4, *B* and *C*, the colocalization of NR2B on the YFP-KIF17 moving vesicles was completely restricted to the dendritic shaft and was totally different from the colocalization of NR2B and PSD95, or NR2B and synaptophysin at synaptic clusters. Furthermore, no colocalization of YFP-KIF17 with NR2B and PSD95 or with NR2B and synaptophysin was observed. Finally, 30.7% ± 5.6% ($n = 40$) of the extrasynaptic NR2B clusters showed clear colocalization with YFP-KIF17 vesicles. On the other hand, we found that at least 44.6 ± 7.1% ($n = 40$) of YFP-KIF17 vesicles are associated with NR2B. The remaining YFP-KIF17, corresponding to vesicles and larger stationary aggregates, did not colocalize with NR2B.

These observations clearly indicate that YFP-KIF17 can transport at least 30% of the NR2B subunits in the dendrites.

Cellular knockdown and functional blockade of KIF17

Furthermore, we wanted to know what will happen if KIF17 is inhibited. To answer this question we performed cellular knockdown of KIF17 by treatment of neuronal cultures with antisense oligonucleotides. Previous studies have successfully demonstrated the inhibition of anterograde transport of tubulovesicular structures using antisense oligonucleotides complementary to the kinesin heavy chain in hippocampal neurons, leading to an alteration in the localization of GAP43 and synapsin I (Ferreira et al., 1992). In this study, we used antisense oligonucleotides against KIF17 to evaluate the effect of its inhibition on the expression level and cellular distribution of NR2B in cultured hippocampal neurons. Antisense or sense oligonucleotides were directly added to the culture medium. We further studied the

expression of KIF17 and NR2B after chronic exposure to antisense oligonucleotides against KIF17, by Western blot analysis of cellular extracts (Fig. 5*A*,*B*). After 3 d of culture, neurons were exposed to 1 μM antisense oligonucleotides, which totally inhibited KIF17 expression and reduced the NR2B expression level by 33.5 ± 2%. After the oligonucleotides were washed out, the expression of both KIF17 and NR2B was restored completely (Fig. 5*A*). Exposure to sense oligonucleotides did not affect the expression level of KIF17 or NR2B. No change in the expression of KIF5B was observed after similar treatments (Fig. 5*A*). In addition, we determined the pattern of expression of several other related proteins, as shown in Figure 5*B*. Exposure to antisense oligonucleotides, which totally inhibited KIF17 expression and reduced the NR2B expression level, also reduced the expression level of mLin10 by 64.3 ± 5.7% (Fig. 5*B*). Surprisingly, antisense treatment increased the NR2A expression level by 24.1 ± 5.2% (Fig. 5*B*). The decrease in the NR2B expression level seemed to be balanced by a parallel increase in the NR2A expression level. Other proteins such as KIF1A, NR2C, PSD95, GluR1, and tubulin were not affected by treatment with antisense oligonucleotides against KIF17 (Fig. 5*B*).

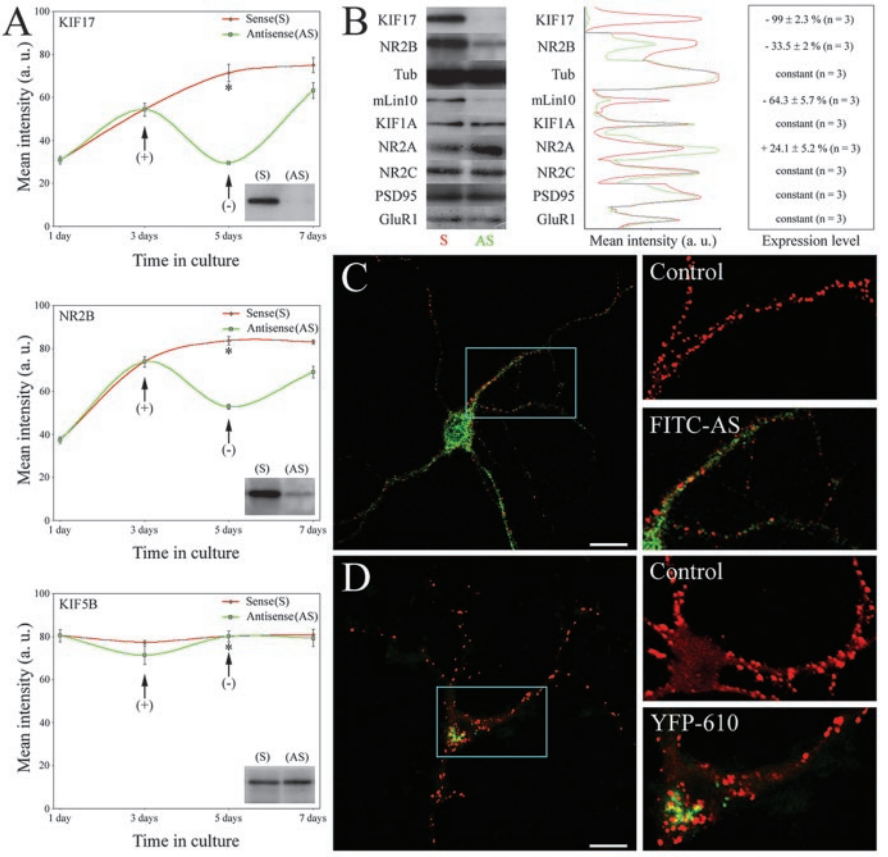

Figure 5. Inhibition of KIF17 in hippocampal neurons. *A*, Inhibition of KIF17 and NR2B expression by antisense oligonucleotide treatment. Hippocampal neurons were exposed (+) to 1 μM antisense or sense oligonucleotides against KIF17 for 3 d. Oligonucleotides were then washed out (−), and neurons were further cultured for 3 more days. After the cells were harvested, 20 μg of protein was separated by PAGE and analyzed by Western blotting with antibodies against KIF17, NR2B, and KIF5B. Bands were detected using ECL, films were scanned, and the bands were quantified using ImageJ. All measurements were standardized on tubulin content. Antisense oligonucleotide treatment (*green curves*) completely inhibited KIF17 expression and also led to a net decrease in the NR2B expression level. No inhibition was observed after sense oligonucleotide treatment (*red curves*). KIF5B expression was not affected by antisense or sense oligonucleotide treatment. After recovery from antisense oligonucleotide treatment, both KIF17 and NR2B expressions were restored. *Insets* on each plot show the bands detected by Western blot analysis (*) after treatment with sense (*S*) or antisense (*A*) oligonucleotides for KIF17, NR2B, and KIF5B. *B*, Western blot analysis of related proteins was performed as described above. Proteins were detected with specific antibodies (see Materials and Methods). Antisense oligonucleotide treatment completely inhibited KIF17 expression and reduced NR2B and mLin10 expression levels by 33 and 64%, respectively. NR2A expression level increased by 24%. No changes in expression level were observed for tubulin, KIF1A, NR2C, PSD95, and GluR1. *C*, Distribution of NR2B in KIF17-knocked-down hippocampal neurons. After 10 d of culture, hippocampal neurons were exposed to 1 μM FITC-tagged antisense oligonucleotides against KIF17. Twenty-four hours later, the cells were fixed, permeabilized, and processed for immunolocalization of NR2B as described in Materials and Methods. NR2B clusters were counted in a 20 μm area. Hippocampal neurons transfected with FITC-tagged antisense oligonucleotides (*green*) showed a marked decrease in the synaptic distribution of NR2B clusters (*red*). Higher magnification of control neurons or neurons exposed to antisense oligonucleotides (*FITC-AS*) is shown. Scale bar, 20 μm. *D*, Distribution of NR2B in dominant-negative overexpressing hippocampal neurons. After 10 d of culture, hippocampal neurons were transfected with YFP-610. Twenty-four hours later, the cells were fixed and processed for immunolocalization of NR2B. Hippocampal neurons transfected with YFP-610 (*green*) showed a similar decrease in the synaptic distribution of NR2B clusters (*red*), as observed after FITC-AS treatment. Note that accumulation of NR2B can be observed in the cell body of YFP-610-transfected neurons. Higher magnification of control neurons or YFP-610-overexpressing neurons is shown. Scale bar, 20 μm.

We then determined the localization of the NR2B subunits in antisense oligonucleotide-treated cultures by using immunofluorescence analysis. Hippocampal neurons were exposed to 1 μM FITC-tagged antisense oligonucleotides for 24 hr. The cells were further fixed and incubated with anti-NR2B antibodies. As shown in Figure 5*C*, neurons transfected with fluorescent antisense oligonucleotides against KIF17 had a 24.8 ± 3.6% ($n = 50$) decrease in the number of synaptic NR2B clusters. Furthermore, an 18.7 ± 3.3% ($n = 50$) increase in the number of synaptic NR2A clusters was observed in antisense oligonucleotide-treated neurons, whereas the number of synaptic NR2C clusters was unchanged (data not shown). Moreover, no similar changes were observed after treatment with fluorescent sense oligonucleotides (data not shown).

We further blocked the activity of KIF17 by overexpression of the dominant-negative mutant YFP-610. Because of the deletion of the motor domain, YFP-610 was restricted to the cell body and did not move into dendrites (data not shown). No changes in the expression level of endogenous KIF17 or NR2B were observed in transfected neurons (data not shown). As observed in Figures 5*D* and 6, neurons expressing YFP-610 had a 22.7 ± 2.1% ($n = 50$) decrease in the number of synaptic NR2B clusters and a 17.8 ± 2.4% ($n = 50$) increase in the number of synaptic NR2A clusters (Fig. 6). A slight accumulation of NR2B clusters occurred in the cell body of the YFP-610-transfected neurons. As observed previously, the number of synaptic NR2C clusters remained identical (Fig. 6). Moreover, the total number of synapses, observed by PSD95 staining, was not affected in any way by the functional blockade of KIF17 (Fig. 6). Only the subunit composition of the NMDARs changed, indicating that KIF17-mediated transport has a preference for NR2B-containing NMDAR vesicles rather than NR2A-containing ones.

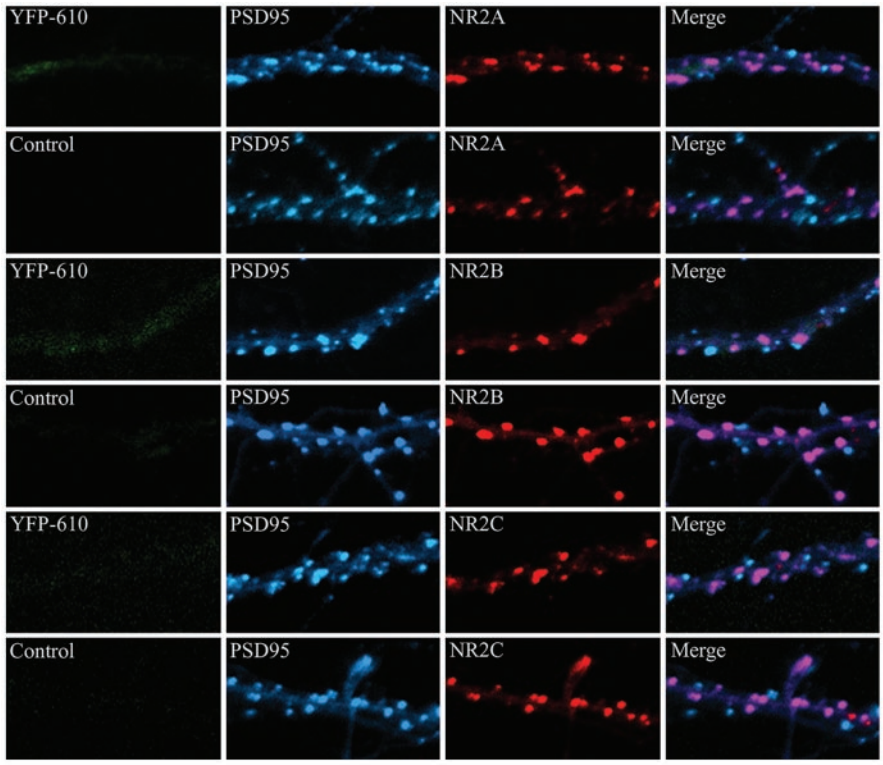

Figure 6. Distribution of NR2 subunits in hippocampal neurons. After 10 d of culture, hippocampal neurons were transfected with YFP-610, fixed, and processed for immunolocalization of NR2A, NR2B, NR2C, and PSD95. The number of positive clusters for each subunit and for PSD95 was counted in a 20 μm area. A 23% decrease in the number of NR2B clusters and an 18% increase in the number of NR2A clusters were observed in neurons overexpressing YFP-610 compared with control nontransfected neurons. No significant changes were observed for NR2C. The total number of PSD95 synaptic clusters did not change.

Taken together, these results reveal a tight coregulation of the expressions of KIF17, NR2B, and mLin10 and that KIF17 is effectively involved in the transport and targeting of NR2B subunits in dendrites. Moreover, these results raise the possibility that one NMDAR subunit, NR2A, can replace and overcome the loss of another subunit, NR2B.

Upregulation of NR2B by pharmacological treatment

To further assess the relationship between KIF17 and NR2B, we focused on their expression level in cultured hippocampal neurons. It has been shown that chronic NMDAR antagonist treatment selectively upregulates NMDAR mRNAs and polypeptides, and more specifically NR2A and NR2B subunits (Follesa and Ticku, 1996; Rao and Craig, 1997). Thus, we wanted to know whether an increase in the NR2B expression level is correlated with an increase in the expression level of its carrier, KIF17. Here we exposed neurons to the NMDAR antagonist AP-V or to the AMPA-type glutamate receptor antagonist CNQX and measured the expression levels of NR2B and KIF17 by Western blot analysis of culture extracts (Fig. 7). The AP-V-treated culture showed a twofold increase in the amount of NR2B after 3–5 d of treatment compared with the control culture treated with CNQX. This result is in agreement with a previous report (Rao and Craig, 1997). Moreover, this increase in the amount of NR2B was correlated with a similar increase in the KIF17 expression level over the same period of time. No difference was observed in the amount of KIF5B between CNQX and AP-V-treated cultures. These results show clearly that the expressions of NR2B and KIF17 are tightly coregulated. The correlation between (1) a higher NR2B expression level, (2) a higher synaptic receptor distribution previously observed by Rao and Craig (1997), and (3) a higher amount of KIF17, shown here, strongly supports the fact that the synaptic redistribution of the NMDAR is mediated in part by the transport of NR2B subunits by KIF17.

Discussion

In this work, we have shown for the first time that the molecular motor KIF17 enters and moves in dendrites of living hippocampal neurons at an average velocity of 0.76 μm/sec. The vesicular structures moved by KIF17 effectively transport NR2B within dendrites, down to the synapses. Moreover, both KIF17 and NR2B expressions seem to be tightly coregulated to efficiently transport and target the receptor subunit to its final synaptic localization.

Movement of KIF17

We characterized the dynamic properties of the molecular motor KIF17 in hippocampal neurons. Our results show clearly that 88.34% of KIF17 moves in dendrites at an average speed of 0.76 μm/sec. Although KIF17 is an anterograde motor, moving from the minus end to the plus end of microtubules, its retrograde movement, observed in the proximal area of the apical dendrite, is only a result of the specific organization of the microtubule network in this area. In fact, microtubules of opposite orientations (plus end and minus end) can be found in this region (Baas et al., 1988), allowing the plus end-directed motor to move in both directions. The significance of this local retrograde movement of KIF17 is not yet known, and KIF17 movement in the dendrite is primarily anterograde, transporting vesicles from the cell body to the tip of the dendrites. The absence of YFP-KIF17 accumulation at the tip of dendrites, as would be expected if KIF17 were continuously transported anterogradely, is unclear. We believe that KIF17 accumulates in several locations in dendrites, excluding the tip. The significance of this accumulation is not yet known, but it is possible that after releasing NR2B, the motor is temporarily stocked before further recycling or degradation. We have no evidence in favor of this hypothesis, however, and further assessment is needed.

The velocity determined here is in agreement with the velocity of KIF17 fast microtubule-dependent transport determined previously *in vitro* (Setou et al., 2000). Moreover, during the preparation of this manuscript, a recent study concerning the dynamic properties of GFP-NR1 has demonstrated that it moves at an average speed of 4 μm/min (Washbourne et al., 2002). Given that NR2 subunits are required for the targeting of NR1 to the synapses (Barria and Malinow, 2002), the velocity of NR1 movement (0.7 μm/sec) and that of KIF17-mediated NR2B movement (0.76 μm/sec) are in good agreement.

Our observations have revealed that the movement of KIF17 is not constant over its entire trajectory: pause, deceleration, or acceleration occurs frequently. Moreover, vesicles in the same area of dendrites do not move at the same velocity. The velocity of molecular motors is probably affected by sev-

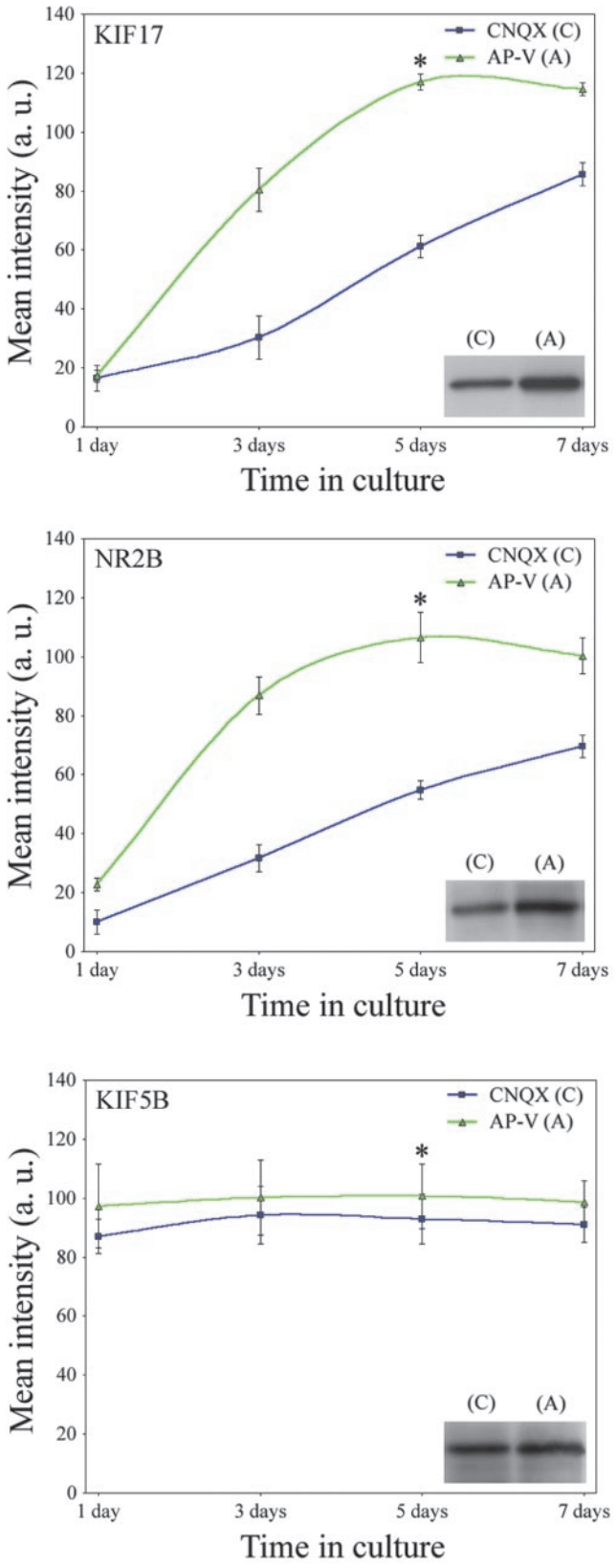

Figure 7. Upregulation of KIF17 and NR2B in neuronal culture. Hippocampal neurons were stimulated with either 100 μM AP-V or 10 μM CNQX up to 7 d of culture. After the cells were harvested, 20 μg of proteins was separated by PAGE and analyzed by Western blotting with antibodies against KIF17, NR2B, and KIF5B. Proteins were detected by ECL, films were scanned, and the bands were quantified using ImageJ. All measurements were standardized on tubulin content. After stimulation with AP-V (*green curves*), a twofold increase in NR2B and KIF17 expression levels was observed, whereas no change in the expression level of KIF5B was observed. KIF17, NR2B, and KIF5B expression levels did not change after CNQX simulation (*blue curves*). *Insets* on each plot show the bands detected by Western blot analysis after 5 d (*) treatment with AP-V (*A*) or CNQX (*C*) for KIF17, NR2B, and KIF5B.

eral intracellular cofactors. It has been shown that the microtubule network interacts with several microtubule-associated proteins (MAPs) and that overexpression of MAPs can inhibit organelle motility and trafficking *in vivo* (Sato-Harada et al., 1996). On the other hand, mapmodulin has been shown to stimulate vesicle transport (Itin et al., 1999). We can assume that similar intracellular interactions and the molecular environment of the motor also probably modulate and regulate the movement of KIF17 along microtubules.

Transport of NR2B

Although endogenous NR2B subunits are dynamically transported, we have not been able to observe directly the movement of exogenous YFP-NR2B in living hippocampal neurons. We believe that technical limitations in our experiments are responsible for this. However, the data presented here have shown that at least 30% of the extrasynaptic NR2B subunits are transported by KIF17. The remaining extrasynaptic NR2B subunits do not seem to be associated with KIF17 and may represent either free NR2B subunits that are already released from the motor and on their way to synaptic clusters or free subunits delivered to the dendritic shaft after synaptic remodeling or turnover and on their way toward recycling or degradation.

We believe that our data concerning (1) the colocalization of endogenous NR2B and YFP-KIF17 on the same vesicle and (2) the functional blockade of KIF17 clearly establish that the effective transport of NR2B is by KIF17. The fraction of endogenous NR2B subunits associated with YFP-KIF17 vesicles move along and stop within the dendritic shaft but do not seem to enter or accumulate in postsynaptic regions. In fact, the actual movement of vesicles through fusion sites within the plasma membrane has not yet been observed. Moreover, such delivery may be too transient to be visualized in our studies. However, these observations raise the possibility that KIF17 only delivers NR2B up to the entrance of synaptic clusters. At this stage, NR2B subunits may change to another protein partner to proceed further and reach their final synaptic destination. Postsynaptic regions are highly enriched in actin filaments (Matus, 2000), and one can assume that these filaments can serve as new tracks for the delivery of NR2B. NMDARs interact with F-actin and myosin light chain (Lei et al., 2001), and it has been proposed but not established that myosin or other actin-based motors can contribute to the transport of glutamate receptors into synapses.

It is important to note that the decrease in the synaptic NR2B observed after antisense oligonucleotide treatment may depend not only on the transport of the subunit but also on the decrease in the expression level of the receptor subunit itself or the scaffolding protein mLin10 as observed by Western blot analysis. A decrease in both transport and expression level of the subunit most likely contributes to the reduction of the synaptic distribution of NR2B.

By using antisense oligonucleotides to knock-down KIF17 or dominant-negative overexpression, we have demonstrated clearly that KIF17 is involved in the transport and correct targeting of NR2B in dendrites. The inhibition in the synaptic localization of NR2B by antisense oligonucleotides against KIF17 gives strong evidence concerning the role of KIF17 in NR2B trafficking. In fact, antisense oli-

gonucleotides or dominant-negative treatment was performed after the initial formation of the neuronal network when most of the synapses were already formed. At that time, synaptic clusters already contained receptors, and we probably inhibited only the transport of the NR2B subunits required during the synaptic turnover of existing synapses or the formation of new synaptic clusters. It has been shown that GFP-PSD95 has a turnover of 20% in 24 hr (Okabe et al., 1999); more recently, the NR1 subunit has been reported to have a turnover of 22% in 16 hr (Vazhappily and Sucher, 2002). According to these data, we can expect a similar turnover of the NR2B subunit, and the inhibition of ~20% in the synaptic localization of NR2B observed in our experiments could be explained by this mechanism. To acquire a general overview of the global effect of KIF17 inhibition on NR2B trafficking, antisense oligonucleotides or dominant-negative treatment should be performed at the early stages of neuronal growth, at least before synaptic formation, or observed in knock-out animal models. Additionally, the decrease in the number of NR2B subunits seems to be compensated by an increase in the number of NR2A subunits. It has been shown that NR2B subunits are replaced by NR2A subunits during development (for review, see Cull-Candy et al., 2001). The increase in the number of NR2A subunits observed in our experiments probably occurs to maintain an appropriate number of functional NMDARs; however, the mechanism of NR2A transport remains to be assessed. Nevertheless, these observations put KIF17 at the center of a complex mechanism that regulates the trafficking and targeting of NR2B subunits; this mechanism needs to be investigated further.

In addition, we have shown the redistribution of the overexpressed mLin10 in neurons cotransfected with KIF17. These results were somehow expected for mLin10 because it was reported previously that mLin10 is part of the scaffolding protein complex involved in the transport of NR2B by KIF17 *in vitro* (Setou et al., 2000); however, these results demonstrate the existence of an interaction between these two proteins.

Expression of KIF17 and NR2B

We have also demonstrated that inhibition of KIF17 expression by chronic exposure to antisense oligonucleotides downregulates the expression of NR2B and mLin10 and upregulates the expression of NR2A. Moreover, after chronic exposure to an NMDAR antagonist, the increase in the amount of NR2B is also correlated to a similar increase in the amount of KIF17. It has been shown that blockade of NMDARs by AP-V upregulates NR2B expression (Follesa and Ticku, 1996). In addition, upregulation of NR2B expression by AP-V treatment enhances the synaptic localization of NMDARs (Rao and Craig, 1997). We can assume that the newly expressed NR2B is then transported to synapses by the newly synthesized KIF17.

Although regulation at the level of protein stability can be involved, we believe that these complementary results indicate the existence of a shared mechanism underlying the transcription of KIF17, NR2B, and mLin10 genes and the expression of their corresponding proteins. This coregulation between a motor and its cargo probably occurs to adequately modulate synaptic activity. Considered together, our data demonstrate the mechanism by which an input controls the ability of a neuron to modify its synapses.

Conclusions

The work presented here describes for the first time the dynamics of KIF17 in living hippocampal neurons and its role in the transport and targeting of NR2B in dendrites. Moreover, our results have also highlighted the close relationship between the expression and distribution of a motor and its cargo. KIF17 clearly appears to be involved in the proper delivery of NR2B at synapses. Inhibition of KIF17 not only leads to major changes in the expression and distribution of NR2B, but also indirectly affects the distribution of NR2A. It appears that KIF17-mediated NR2B trafficking is one of the key regulators of NMDAR formation in living hippocampal neurons. Finally, the important role of NR2B in neuronal plasticity, learning, and memory indicates the need to further understand and study how KIF17 can contribute and modulate the expression, localization, and activity of NR2B and NMDARs in animal models.

References

Baas PW, Deitch JS, Black MM, Banker GA (1988) Polarity orientation of microtubules in hippocampal neurons: uniformity in the axon and nonuniformity in the dendrite. Proc Natl Acad Sci USA 85:8335–8339.

Barria A, Malinow R (2002) Subunit-specific NMDA receptor trafficking to synapses. Neuron 35:345–353.

Bliss TV, Collingridge GL (1993) A synaptic model of memory: long-term potentiation in the hippocampus. Nature 361:31–39.

Burack MA, Silverman MA, Banker G (2000) The role of selective transport in neuronal protein sorting. Neuron 26:465–472.

Craven SE, El-Husseini AE, Bredt DS (1999) Synaptic targeting of the postsynaptic density protein PSD-95 mediated by lipid and protein motifs. Neuron 22:497–509.

Cull-Candy S, Brickley S, Farrant M (2001) NMDA receptor subunits: diversity, development and disease. Curr Opin Neurobiol 11:327–335.

Ferreira A, Niclas J, Vale RD, Banker G, Kosik KS (1992) Suppression of kinesin expression in cultured hippocampal neurons using antisense oligonucleotides. J Cell Biol 117:595–606.

Fischer M, Kaech S, Knutti D, Matus A (1998) Rapid actin-based plasticity in dendritic spines. Neuron 20:847–854.

Follesa P, Ticku MK (1996) NMDA receptor upregulation: molecular studies in cultured mouse cortical neurons after chronic antagonist exposure. J Neurosci 16:2172–2178.

Forrest D, Yuzaki M, Soares HD, Ng L, Luk DC, Sheng M, Stewart CL, Morgan JI, Connor JA, Curran T (1994) Targeted disruption of NMDA receptor 1 gene abolishes NMDA response and results in neonatal death. Neuron 13:325–338.

Gho M, McDonald K, Ganetzky B, Saxton WM (1992) Effects of kinesin mutations on neuronal functions. Science 258:313–316.

Goslin K, Banker G (1991) Rat hippocampal neurons in low-density culture. In: Culturing nerve cells (Banker G, Goslin K, eds), pp 251–281. Cambridge, MA: MIT.

Hirokawa N (1996) Organelle transport along microtubules–the role of KIFs (kinesin superfamily proteins). Trends Cell Biol 6:135–141.

Hirokawa N (1998) Kinesin and dynein superfamily proteins and the mechanism of organelle transport. Science 279:519–526.

Itin C, Ulitzur N, Muhlbauer B, Pfeffer SR (1999) Mapmodulin, cytoplasmic dynein, and microtubules enhance the transport of mannose 6-phosphate receptors from endosomes to the *trans*-Golgi network. Mol Biol Cell 10:2191–2197.

Kanai Y, Okada Y, Tanaka Y, Harada A, Terada S, Hirokawa N (2000) KIF5C, a novel neuronal kinesin enriched in motor neurons. J Neurosci 20:6374–6384.

Kohrmann M, Haubensak W, Hemraj I, Kaether C, Lessmann VJ, Kiebler MA (1999a) Fast, convenient, and effective method to transiently transfect primary hippocampal neurons. J Neurosci Res 58:831–835.

Kohrmann M, Luo M, Kaether C, DesGroseillers L, Dotti CG, Kiebler MA (1999b) Microtubule-dependent recruitment of Staufen-green fluorescent protein into large RNA-containing granules and subsequent dendritic transport in living hippocampal neurons. Mol Biol Cell 10:2945–2953.

Kutsuwada T, Kashiwabuchi N, Mori H, Sakimura K, Kushiya E, Araki K, Meguro H, Masaki H, Kumanishi T, Arakawa M, Mishina M (1992) Molecular diversity of the NMDA receptor channel. Nature 358:36–41.

Laemmli UK (1970) Cleavage of structural proteins during the assembly of the head of bacteriophage T4. Nature 227:680–685.

Lei S, Czerwinska E, Czerwinski W, Walsh MP, MacDonald JF (2001) Regulation of NMDA receptor activity by F-actin and myosin light chain kinase. J Neurosci 21:8464–8472.

Matus A (2000) Actin-based plasticity in dendritic spines. Science 290: 754–758.

Miki H, Setou M, Kaneshiro K, Hirokawa N (2001) All kinesin superfamily protein, KIF, genes in mouse and human. Proc Natl Acad Sci USA 98:7004–7011.

Monyer H, Sprengel R, Schoepfer R, Herb A, Higuchi M, Lomeli H, Burnashev N, Sakmann B, Seeburg PH (1992) Heteromeric NMDA receptors: molecular and functional distinction of subtypes. Science 256:1217–1221.

Mori H, Manabe T, Watanabe M, Satoh Y, Suzuki N, Toki S, Nakamura K, Yagi T, Kushiya E, Takahashi T, Inoue Y, Sakimura K, Mishina M (1998) Role of the carboxy-terminal region of the GluR epsilon2 subunit in synaptic localization of the NMDA receptor channel. Neuron 21:571–580.

Moriyoshi K, Masu M, Ishii T, Shigemoto R, Mizuno N, Nakanishi S (1991) Molecular cloning and characterization of the rat NMDA receptor. Nature 354:31–37.

Nakagawa T, Tanaka Y, Matsuoka E, Kondo S, Okada Y, Noda Y, Kanai Y, Hirokawa N (1997) Identification and classification of 16 new kinesin superfamily (KIF) proteins in mouse genome. Proc Natl Acad Sci USA 94:9654–9659.

Okabe S, Kim HD, Miwa A, Kuriu T, Okado H (1999) Continual remodeling of postsynaptic density and its regulation by synaptic activity. Nat Neurosci 2:804–811.

Okamoto M, Sudhof TC (1997) Mints, Munc18-interacting proteins in synaptic vesicle exocytosis. J Biol Chem 272:31459–31464.

Prekeris R, Foletti DL, Scheller RH (1999) Dynamics of tubulovesicular recycling endosomes in hippocampal neurons. J Neurosci 19:10324–10337.

Rao A, Craig AM (1997) Activity regulates the synaptic localization of the NMDA receptor in hippocampal neurons. Neuron 19:801–812.

Rongo C, Whitfield CW, Rodal A, Kim SK, Kaplan JM (1998) LIN-10 is a shared component of the polarized protein localization pathways in neurons and epithelia. Cell 94:751–759.

Sakimura K, Kutsuwada T, Ito I, Manabe T, Takayama C, Kushiya E, Yagi T, Aizawa S, Inoue Y, Sugiyama H, Mishina M (1995) Reduced hippocampal LTP and spatial learning in mice lacking NMDA receptor epsilon 1 subunit. Nature 373:151–155.

Sato-Harada R, Okabe S, Umeyama T, Kanai Y, Hirokawa N (1996) Microtubule-associated proteins regulate microtubule function as the track for intracellular membrane organelle transports. Cell Struct Funct 21:283–295.

Setou M, Nakagawa T, Seog DH, Hirokawa N (2000) Kinesin superfamily motor protein KIF17 and mLin10 in NMDA receptor-containing vesicle transport. Science 288:1796–1802.

Shi SH, Hayashi Y, Petralia RS, Zaman SH, Wenthold RJ, Svoboda K, Malinow R (1999) Rapid spine delivery and redistribution of AMPA receptors after synaptic NMDA receptor activation. Science 284:1811–1816.

Tang YP, Shimizu E, Dube GR, Rampon C, Kerchner GA, Zhuo M, Liu G, Tsien JZ (1999) Genetic enhancement of learning and memory in mice. Nature 401:63–69.

Tsien JZ, Huerta PT, Tonegawa S (1996) The essential role of hippocampal CA1 NMDA receptor-dependent synaptic plasticity in spatial memory. Cell 87:1327–1338.

Vazhappily R, Sucher NJ (2002) Turnover of *N*-methyl-D-aspartate receptor subunit NR1 in PC12 cells. Neurosci Lett 318:153–157.

Washbourne P, Bennett JE, McAllister AK (2002) Rapid recruitment of NMDA receptor transport packets to nascent synapses. Nat Neurosci 5:751–759.

White J, Stelzer E (1999) Photobleaching GFP reveals protein dynamics inside live cells. Trends Cell Biol 9:61–65.

Yang Z, Hanlon DW, Marszalek JR, Goldstein LS (1997) Identification, partial characterization, and genetic mapping of kinesin-like protein genes in mouse. Genomics 45:123–131.

Zhao C, Takita J, Tanaka Y, Setou M, Nakagawa T, Takeda S, Yang HW, Terada S, Nakata T, Takei Y, Saito M, Tsuji S, Hayashi Y, Hirokawa N (2001) Charcot-Marie-Tooth disease type 2A caused by mutation in a microtubule motor KIF1Bbeta. Cell 105:587–597.